QUARTERLY JOURNAL OF THE ROYAL METEOROLOGICAL SOCIETY
Q. J. R. Meteorol. Soc. **135**: 1661–1672 (2009)
Published online 29 September 2009 in Wiley InterScience
(www.interscience.wiley.com) DOI: 10.1002/qj.479

A critical comparison of stratosphere–troposphere coupling indices

Mark P. Baldwin[a]* and David W.J. Thompson[b]
[a]*NorthWest Research Associates, Redmond, Washington, USA*
[b]*Department of Atmospheric Science, Colorado State University, Fort Collins, Colorado, USA*

ABSTRACT: Assessing stratosphere–troposphere coupling in observational data or model output requires a multi-level index with high time resolution. Ideally, such an index would (1) represent spatial patterns in the troposphere that are most strongly coupled with stratospheric variability and (2) be robust and computationally feasible in both observations and standard model output.

Several of the indices used to diagnose extratropical stratosphere–troposphere coupling are based on the Northern and Southern Hemisphere annular modes. The annular mode indices are commonly defined as the leading empirical orthogonal functions (EOFs) of monthly-mean, hemispheric geopotential height. In the lowermost troposphere, the structure of the annular modes is defined as the leading EOF of the near-surface geopotential height field, and these patterns correspond well to the patterns of variability induced by stratospheric circulation changes. At pressure levels above the surface, the structure of the annular modes is typically found by either calculating the local EOF or regressing geopotential height data onto the leading principal component time series of near-surface geopotential height.

Here we make a critical comparison of the existing methodologies used to diagnose stratosphere–troposphere coupling, including EOF-based indices as well as measures based on zonal-mean wind at a fixed latitude and geopotential height over the polar cap. We argue in favour of an alternative methodology based on EOFs of daily zonally-averaged geopotential. We find that (1) the daily evolution of stratosphere–troposphere coupling events is seen most clearly with this methodology, and (2) the methodology is robust and requires few subjective choices, making it readily applicable to climate model output available only in zonal-mean form.

KEY WORDS annular modes; NAM; EOF

Received 6 February 2009; Revised 6 May 2009; Accepted 23 June 2009

1. Introduction

The Northern and Southern Hemisphere annular modes (NAM and SAM) are the dominant forms of dynamic variability in their respective hemispheres, and indices of the annular modes are frequently used as climate diagnostics. The spatial structure of the annular modes is commonly defined as the leading empirical orthogonal function (EOF) of near-surface, monthly-mean geopotential anomalies poleward of 20°, and temporal variability in the annular modes is often defined as the corresponding leading Principal Component (PC) time series (e.g. Kidson, 1988; Karoly, 1990; Thompson and Wallace, 1998, 2000; Limpasuvan and Hartmann, 2000; Quadrelli and Wallace, 2004). However, a number of alternative methods are also in wide use in the literature, depending on the application. For example, Baldwin and Dunkerton (2001) generated annular mode indices at daily resolution and as a function of vertical level by projecting daily data onto the leading EOFs of monthly-mean geopotential height anomalies calculated separately at all levels. Hurrell *et al.* (2003) defined the NAM as the leading EOF of the sea-level pressure (SLP, equivalent to 1000 hPa geopotential) field over the North Atlantic sector. Kidson (1988), Hartmann and Lo (1998) and Lorenz and Hartmann (2001, 2003) defined the annular modes as the leading EOFs of extratropical zonal-mean zonal wind. Gong and Wang (1999) and Marshall (2003) defined the SAM as the linear difference between pressures averaged along approximately 65°S and 40°S, whilst Li and Wang (2003) and Braesicke and Pyle (2004) used similar zonally averaged SLP differences in the Northern Hemisphere. Christiansen (2005, 2009) defined annular variability as the zonal-mean wind along 60° latitude.

Each of the existing methodologies offers advantages for calculating annular modes. The daily height–time indices from Baldwin and Dunkerton (2001), based on EOFs calculated separately at each level, facilitate better understanding of vertical coupling of the stratosphere and troposphere, and they make possible the calculation of a wide variety of vertically varying diagnostics, such as the e-folding time-scale and variance of the annular modes (e.g. Norton, 2003; Gerber *et al.*, 2008a, 2008b). The EOFs of the North Atlantic sector are useful for analysing dynamics local to the North Atlantic storm track. The

*Correspondence to: M.P. Baldwin, NorthWest Research Associates, 4118 148th Ave NE, Redmond, WA 98052, USA.
E-mail: mark@nwra.com

EOFs of zonal-mean zonal wind used in Hartmann and Lo (1998) and Lorenz and Hartmann (2001) provide time indices which can be used to quantitatively assess the relationships between the eddy momentum fluxes and the tendency of the zonal-mean zonal flow. The use of data along fixed latitudes, for example, SLP along 65°S and 40°S (Gong and Wang, 1999; Marshall, 2003) or the zonal wind along 60°N (Christiansen, 2005, 2009), simplifies the calculation of the annular mode indices and can be done using sparse station data.

But there are also drawbacks to the current methodologies, particularly with regard to analysing deep vertical coupling of the annular modes. The first EOF of the upper tropospheric Northern Hemisphere geopotential height field (as used in Baldwin and Dunkerton (2001)) is not purely indicative of annular variability in the free troposphere, but reflects variability due to both the NAM and the Pacific–North American (PNA) pattern (Quadrelli and Wallace, 2004). Regional EOFs are inevitably sensitive to the longitudinal boundaries used in the analysis. The middle latitude centre of action of the SAM in the pressure field is located ∼50° latitude (i.e. not 40° latitude, as used in some studies), and the latitude of the polar centre of action of the annular modes in the zonal wind field varies between the stratosphere and the troposphere.

Finally, the calculation of multi-level daily annular mode indices requires a large data volume – decades of daily three-dimensional hemispheric data. This is not an issue for observations, such as reanalyses from the National Centers for Environmental Prediction (NCEP) and the European Centre for Medium-range Weather Forecasts (ECMWF). However, the required data volume can be an impediment to obtaining daily, multi-level annular mode indices from long model simulations. Typically, daily latitude–longitude maps of geopotential at many levels are not archived in long climate simulations, making impossible the calculation of daily annual mode indices based on existing methods. For example, the archived output from the Intergovernmental Panel on Climate Change (IPCC) AR4 models is provided only in monthly-mean form, making it possible to assess long-term trends in the annular modes (Miller *et al.*, 2006), but not diagnostics of stratosphere–troposphere coupling.

Here we critically assess the existing methodologies used to diagnose stratosphere–troposphere coupling. Based on the results, we argue that the daily evolution of stratosphere–troposphere coupling events is clearest and most readily assessed from the leading PC time series of daily-mean, zonal-mean, year-round geopotential height calculated as a function of vertical level. The method requires few subjective choices and modest data volume, and the resulting indices are more strongly vertically coupled than any other set of indices currently used for assessing stratosphere–troposphere coupling. In section 2 we outline the existing methodologies and the proposed recipe. In section 3 we compare results from the proposed recipe with those based on existing methodologies. In section 4 we discuss the implications of the proposed recipe for the analysis of observed and simulated variability in the annular modes.

2. Calculation of annular mode indices

In this section we outline two existing methods for calculating the spatial patterns and indices of the NAM and the SAM. We then detail a third method based on zonal-mean, daily-mean data. The geopotential data, Z, for a given pressure level, are organized in an $(n \times p)$ matrix, $Z = [z_1, z_2, \ldots, z_n]^{\mathrm{T}}$, containing n observations in time of geopotential z_i defined at p spatial points, typically a latitude–longitude grid. The seasonal cycle is removed from the data and the time mean of the data at each grid point is zero. The subscript l indicates pressure level, and superscripts d and m denote daily and monthly-mean data.

2.1. Relationship between EOFs and data projections

Let e denote a p-vector spatial pattern and y denote an n-vector time series of centred anomalies. For example, a data matrix Z can be written as a sum of the products of EOFs $\{e_1, e_2, \ldots\}$ and PC time series $\{y_1, y_2, \ldots\}$:

$$Z = \sum_{i=1}^{r} y_i e_i^{\mathrm{T}}$$

where r is the rank of Z. An EOF can be obtained from a PC time series by regressing the data onto the time series:

$$e = \frac{Z^{\mathrm{T}} y}{y^{\mathrm{T}} y} \tag{1}$$

More generally, (1) can be used to obtain a spatial pattern from any dataset and time series that have the same time dimension.

Similarly, a time series y can be obtained from a spatial pattern e by projecting the data onto the spatial pattern. This procedure can incorporate spatial weighting to compensate for unequal grid boxes (e.g. North *et al.*, 1982; Baldwin *et al.*, 2009). We define W as a p vector with elements a_i proportional to the area of each grid box (cosine of latitude for a latitude–longitude grid). A time series can be obtained by projecting a data matrix onto a spatial pattern by:

$$y = \frac{ZWe}{e^{\mathrm{T}} We} \tag{2}$$

In the discussions below, we will use (1) to regress data onto time series, and (2) to project data onto spatial patterns.

2.2. Method number one: Surface-based EOFs

The *surface-based* method for defining an annular mode spatial pattern and a corresponding index is based on EOF analysis of monthly-mean lower tropospheric geopotential height (Thompson and Wallace, 1998, 2000). The analysis may include all months, or it may be restricted to a select season (e.g. to winter months in the Northern Hemisphere). The NAM is defined as the leading EOF of

DOI: 10.1002/qj

Z^m_{1000} and the NAM index as the corresponding PC time series y^m_{1000} (the SAM is defined in an analogous manner but is typically based instead on 850 or 500 hPa height). To find the structure of the annular mode at other pressure levels, Z fields are regressed onto y^m_{1000} using (1):

$$e^m_p = \frac{Z^m_p y^m_{1000}}{(y^m_{1000})^{\mathrm{T}}\, y^m_{1000}} \tag{3}$$

A daily, year-round, NAM index can be constructed by projecting daily 1000 hPa geopotential Z^d_{1000} onto the NAM pattern e^m_{1000} using (2):

$$y^d_{1000} = \frac{Z^d_{1000} W e^m_{1000}}{(e^m_{1000})^{\mathrm{T}} W e^m_{1000}} \tag{4}$$

There are several downsides to the above methodology for assessing stratosphere–troposphere coupling. First, the method does not necessarily capture annular variability in the middle stratosphere. This is because the EOFs of the troposphere are not the best metric for defining stratospheric annular variability, and it is also because the regression in (3) does not account for the time-lag between variability in the middle stratospheric and surface flow. Second, the regression in (3) is sensitive to the seasons used in the analysis, particularly when generating the structure of the annular modes at stratospheric levels. Third, the generation of daily-resolution indices at a given level l is cumbersome, as it requires first calculating the leading PC time series of the monthly-mean surface geopotential height field, regressing monthly-mean geopotential height data at level l onto the resulting leading PC time series index to obtain spatial maps at each level, and then projecting daily-mean geopotential height data at level l onto the corresponding regression map.

2.3. Method number two: Height-dependent EOFs

The *height-dependent* method is the same as the *surface-based* method at 1000 hPa, but at all other levels the annular mode is defined as the leading EOF of monthly-mean, zonally-varying, geopotential height at that pressure level (Baldwin and Dunkerton, 2001). We denote e^m_l as the EOF (NAM or SAM pattern) at pressure level l, and y^m_l as the PC time series (NAM or SAM index with monthly resolution). Daily indices are obtained at each pressure level by projecting daily geopotential data Z^d_l onto the spatial patterns e^m_l using (2):

$$y^d_l = \frac{Z^d_l W e^m_l}{(e^m_l)^{\mathrm{T}} W e^m_l} \tag{5}$$

The main downsides of the height-dependent methodology for assessing stratosphere–troposphere coupling are that (1) the method is computationally expensive, as it requires daily-mean geopotential maps at all levels, and (2) in the Northern Hemisphere upper troposphere, the leading EOF is not representative of the pattern most strongly associated with stratospheric variability, but rather it is a mix of annular variability and the Pacific–North American pattern (Quadrelli and Wallace, 2004).

2.4. Method number three: Zonal-mean EOFs

The third methodology for assessing stratosphere–troposphere coupling is similar to the height-dependent method used in Baldwin and Dunkerton (2001), but is based on daily averaged, *zonally averaged*, year-round geopotential height, $\overline{Z^d_l}$. The method is an extension of the zonal-mean EOFs calculated for SLP data in Baldwin (2001), and for a single level of geopotential in Gerber *et al.* (2008a). The daily zonal-mean NAM or SAM indices are the PC time series $\overline{y^d_l}$, but the EOFs $\overline{e^d_l}$ are functions of latitude only. The zonally varying NAM and SAM patterns at each pressure level are found by regressing either daily-mean geopotential height data Z^d_l onto the daily mean values of $\overline{y^d_l}$ or, as done in the following section, monthly-mean geopotential height Z^m_l data onto monthly mean values of $\overline{y^d_l}$. In the latter case, the monthly-mean time series are constructed by taking monthly means of the daily PC time series (the monthly-mean time series are denoted $[\overline{y^d_l}]$), and the maps are obtained as:

$$e^m_l = \frac{Z^m_l \overline{[y^d_l]}}{([y^d_l])^T [y^d_l]} \tag{6}$$

As demonstrated in the following section, the zonal-mean EOFs are not burdened by the downsides associated with the first two methods. At all levels in both hemispheres the zonal-mean EOFs yield structures consistent with annular variability (in contrast to the multi-level method in the Northern Hemisphere troposphere), the stratospheric structures are not dependent on defining a time-lag between the surface and stratospheric flow (in contrast to the surface-based method), and the proposed recipe provides daily resolution indices as a function of height with relatively few computations and few subjective choices.

3. Results

In this section we compare the spatial patterns and time series derived from the three methods outlined in section 2. The comparisons reveal the consistency among all three methods, but also highlight the disadvantages of using the surface-based and multi-level methods for assessing stratosphere–troposphere coupling.

All the results are based on the ECMWF ERA-40 reanalysis and operational data spanning 1958 to 2007. The ERA-40 data (Uppala *et al.*, 2005) consist of daily averages of geopotential on a 1.125° latitude–longitude grid, at 23 standard pressure levels from 1000 to 1 hPa for the period January 1958 to August 2002 (http://www.ecmwf.int/research/era), and the operational data archive extends the ERA-40 reanalysis after that date. Where necessary, the seasonal cycle was removed from daily data by subtracting the 90-day low-pass filtered values for each day at each grid point. The seasonal cycle was removed from monthly-mean data by subtracting the mean values for each month.

DOI: 10.1002/qj

The definition of the leading EOF is not sensitive to the precise position of the equatorward boundary. We calculated the zonal-mean daily NAM index for all data levels between 1000 and 3 hPa using equatorward boundaries of 0°, 10°N, 20°N, and 30°N. At each level, correlations between these indices were generally above 0.999 and never below 0.995. For all the calculations below we used the Equator as the boundary.

Stratospheric variability tends to induce annular tropospheric patterns (e.g. Baldwin and Dunkerton, 2001; Thompson and Solomon, 2002). In Figure 1 we show the 1000 and 300 hPa height patterns associated with deep wintertime (November to March) stratospheric wind anomalies at 60°N. The left column shows regression patterns based on standardized values of zonal-mean zonal wind anomalies averaged over 100–3 hPa at 60°N. The right two columns are composites based on days when the vertically averaged wind between 100 and 3 hPa exceeds ± 5 m s^{-1}, a criterion that includes more than 20% of all days during winter in each category. The patterns derived from the regressions and composites are effectively identical, which indicates that they are robust to the details of the analysis, e.g. the stratospheric wind threshold, months used and time-lags. They are also linear, in the sense that the patterns corresponding to weak stratospheric winds closely resemble the opposite of those corresponding to strong stratospheric winds. The patterns in the middle column resemble closely the tropospheric anomalies observed 0–60 days following sudden stratospheric warmings (Baldwin and Dunkerton, 2001). The patterns in Figure 1 may be viewed as a benchmark for determining the effectiveness of the methods outlined in section 2 for assessing the tropospheric patterns most closely associated with stratospheric variability.

Figure 2 examines the spatial structure of the NAM at 1000, 300, 30 and 3 hPa for the three methods described in section 2. The data used are year-round monthly mean geopotential anomalies, with a latitudinal domain from the Equator to the Pole. By definition, the positive polarity of the annular mode has a negative geopotential height anomaly over the polar cap. The left column shows the structure of the NAM as derived from the surface-based methodology (i.e. regressions onto the leading PC time series of 1000 hPa geopotential height), the middle column shows the structure of the NAM as derived from the height-dependent methodology (i.e. regressions onto the leading PC time series of geopotential height calculated separately at all levels), and the right column shows the structure of the NAM as derived from the proposed zonal-mean methodology. In the case of the zonal-mean methodology, we show regressions onto monthly means of the daily PC time series, as given by equation (6).

By construction, at 1000 hPa the first two methods yield identical patterns (i.e. both correspond to the regression of 1000 hPa geopotential height onto the leading PC of the zonally varying 1000 hPa geopotential field).

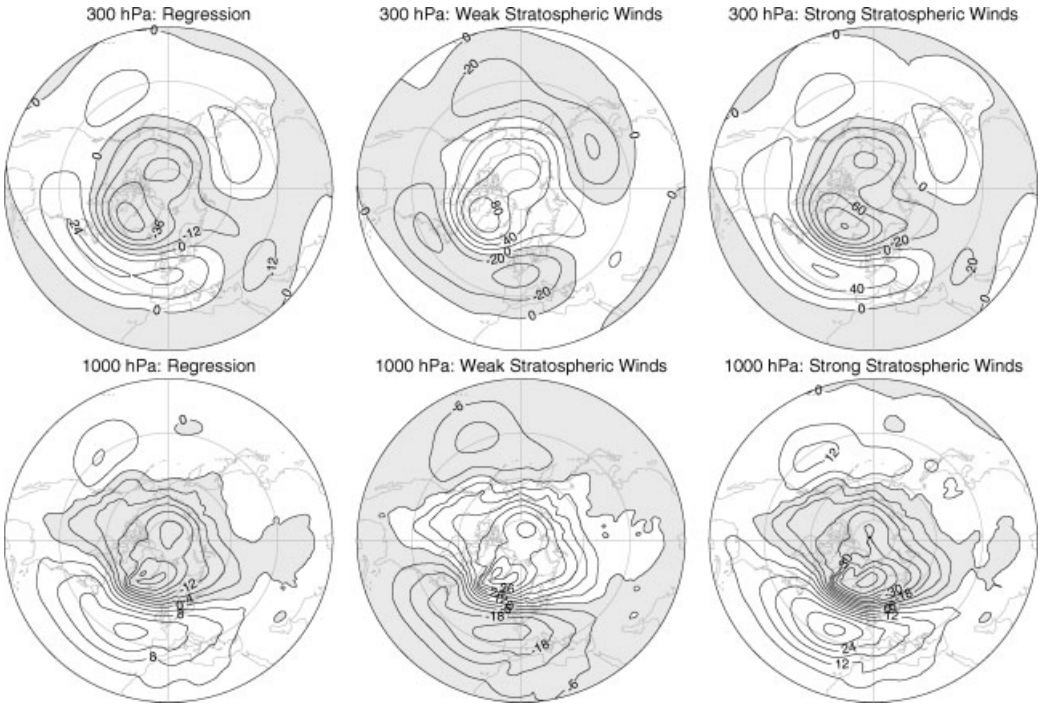

Figure 1. Left column: 300 and 1000 hPa regressions between daily stratospheric wind anomalies at 60°N (log-pressure averaged from 100 to 3 hPa), during winter days (November–March). Right two columns: Average tropospheric geopotential anomaly patterns during winter days (November-March) with anomalously weak (left column) and strong (right column) stratospheric winds. Days with anomalously weak stratospheric winds are defined by negative zonal-mean wind anomalies at all levels between 100 and 3 hPa, with a mean value less than −5 m s^{-1}. Similarly, anomalously strong stratospheric winds are defined by positive zonal-mean wind anomalies at all levels between 100 and 3 hPa, with mean values greater than 5 m s^{-1}. Twenty-two percent of the winter days met the definition of weak stratospheric winds, whilst 20% met the definition of strong stratospheric winds. Thus, each panel represents the average of over 4500 days of data. The area-weighted spatial correlation between left and right panels is −0.96 at 300 hPa, and it is −0.94 at 1000 hPa.

DOI: 10.1002/qj

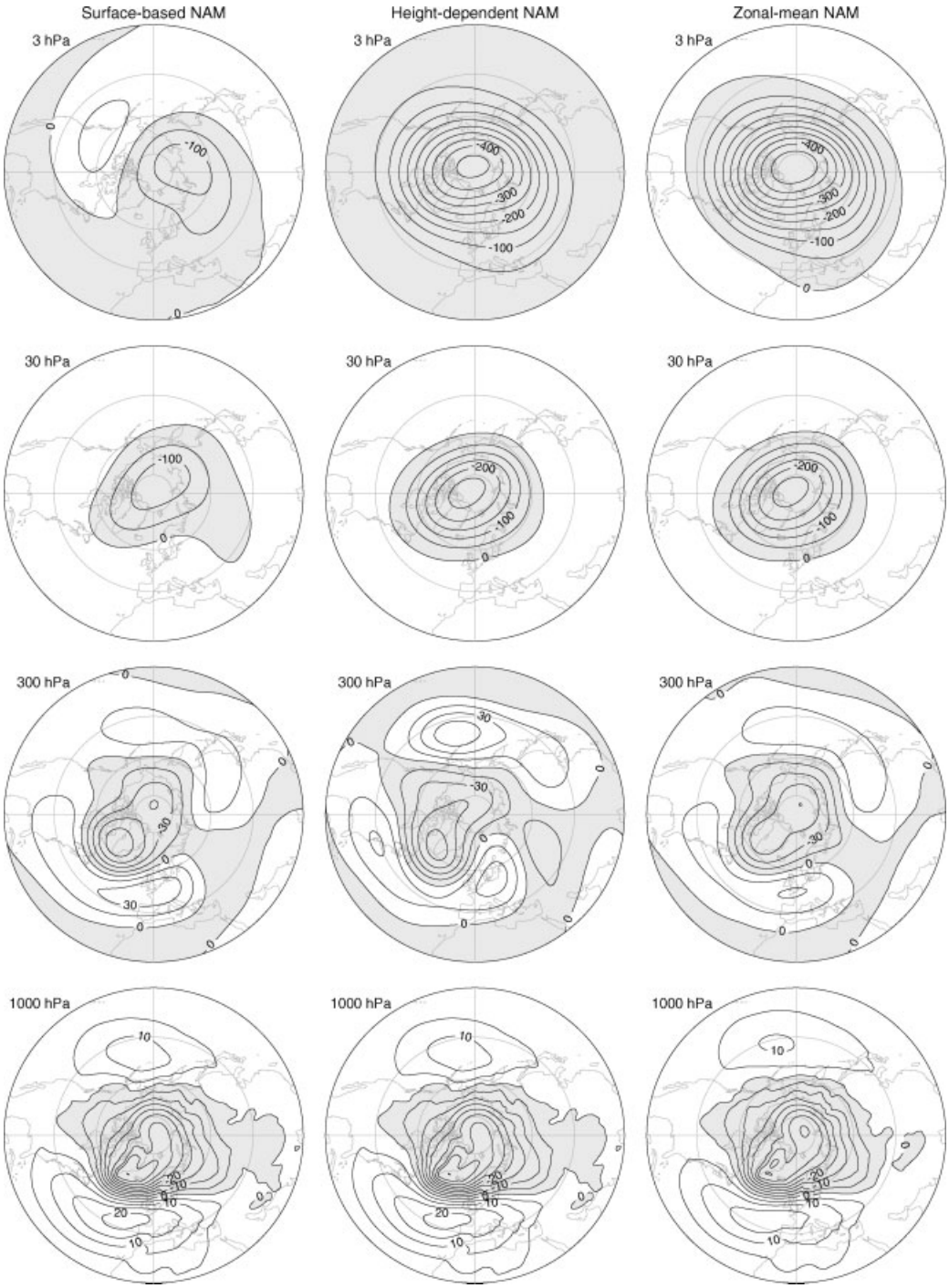

Figure 2. Left column: Spatial patterns of the surface-based NAM, with a base level of 1000 hPa, defined using equation (3) (Thompson and Wallace, 1998, 2000). Centre column: spatial patterns (EOFs) of the height-dependent NAM (Baldwin and Dunkerton, 2001). Right column: spatial patterns of the zonal-mean NAM, defined using equation (6).

The pattern associated with the zonal-mean methodology (right panel) has comparatively weak amplitude over the North Atlantic sector, but otherwise is largely identical to the patterns in the middle and left panels (the area-weighted spatial correlation between pairs of patterns is shown in Table I). Hence, as discussed in Thompson and Wallace (2000), at the surface the dominant forms of variability in the zonal-mean and zonally varying circulations are largely indistinguishable from each other. All patterns are very similar to the observed patterns of 1000 hPa anomalies shown in the bottom row of Figure 1, and thus all methods outlined in section 2 capture the pattern of near-surface variability associated with shifts in the strength of stratospheric winds.

The differences among the three methods are more pronounced at the 300 hPa level. The pattern derived from the surface-based EOF (left panel) of Figure 2 is more wave-like than its surface counterpart, with enhanced amplitude over the North Atlantic sector. The pattern obtained from the height-dependent EOF (middle

DOI: 10.1002/qj

Table I. Area-weighted spatial correlations between pairs of panels in Figure 2.

	Columns 1–2	Columns 1–3	Columns 2–3
3 hPa	0.414	0.432	0.996
30 hPa	0.889	0.905	0.999
300 hPa	0.853	0.944	0.803
1000 hPa	1.00	0.996	0.996

panel) of Figure 2 is more zonally asymmetric, with substantial distortions from zonal symmetry found over both the North Atlantic and Pacific sectors. The zonal-mean EOF (right panel) of Figure 2 provides the most zonally symmetric pattern and hence structurally most resembles its surface counterpart. Both the surface-based NAM and the zonal-mean NAM patterns correspond closely to the observed 300 hPa anomalies illustrated in Figure 1, indicating that both methods strongly resemble the pattern of tropospheric variability associated with shifts in the strength of stratospheric winds. In contrast, the height-dependent NAM is much more wave-like than the 300 hPa pattern shown in Figure 1.

The differences among the patterns at 300 hPa can be interpreted as follows. In the case of the left column, the pattern at 300 hPa reflects the juxtaposition of zonally symmetric variability in the NAM and a wave-like structure induced by temperature advection by the zonal mean flow at the surface (Thompson and Wallace, 2000). Cold advection over eastern North America and warm advection over central Asia drive thickness anomalies that give rise to the trough to the west of Greenland and the ridges over Europe and eastern Asia.

In the case of the middle column, the pattern at 300 hPa is contaminated by the second EOF of the SLP field, and is thus a mix of the NAM and the PNA (Quadrelli and Wallace, 2004). That this is the case is exemplified in Figure 3. The top panels in Figure 3 show the patterns found by regressing the 300 hPa geopotential height field onto the first (left) and second (right) PC time series of the 1000 hPa geopotential height field. Hence, the top left panel in Figure 3 is a repeat of the surface-based NAM at 300 hPa from Figure 2, while the top right panel shows analogous results for the surface-based PNA at 300 hPa, assuming the PNA corresponds to the second EOF/PC pair of the 1000 hPa height field (see Quadrelli and Wallace, 2004). The bottom panels in Figure 3 compare

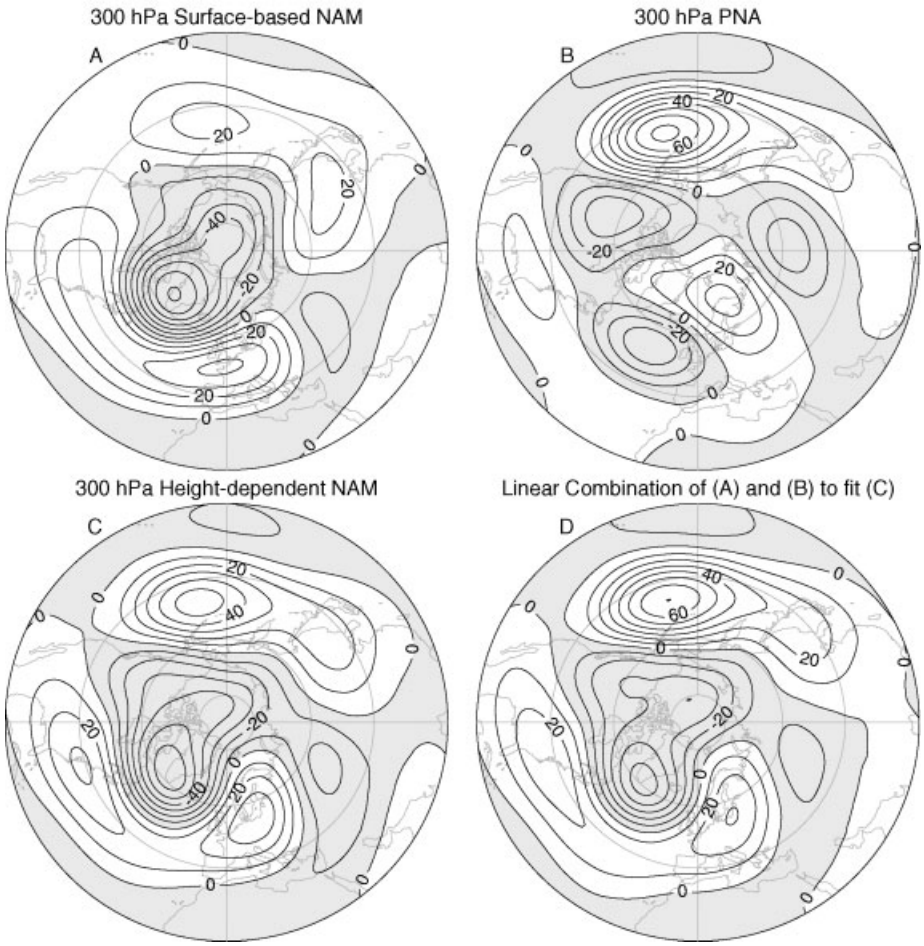

Figure 3. (A) 300 hPa surface-based NAM, calculated by regressing monthly-mean 300 hPa geopotential onto the time series of the first EOF at 1000 hPa (as in Figure 1). (B) 300 hPa PNA pattern, calculated by regressing monthly-mean 300 hPa geopotential onto the time series of the second EOF at 1000 hPa. (C) 300 hPa height-dependent NAM (as in Figure 1). (D) Optimum linear combination of (A) and (B) to fit (C). The spatial correlation between (C) and (D) is 0.98.

DOI: 10.1002/qj

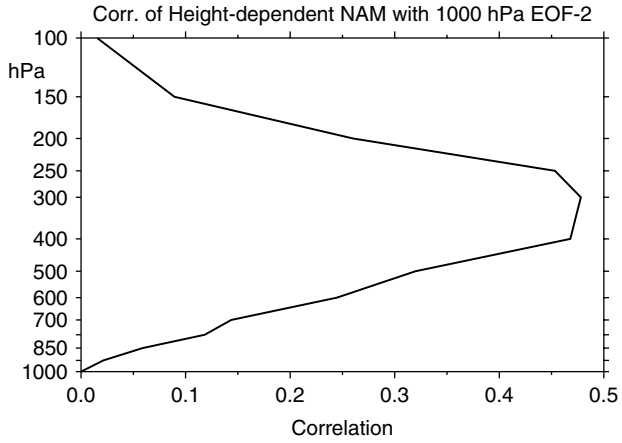

Figure 4. Correlations between the PC time series of the second EOF at 1000 hPa with the height-dependent NAM index as a function of pressure.

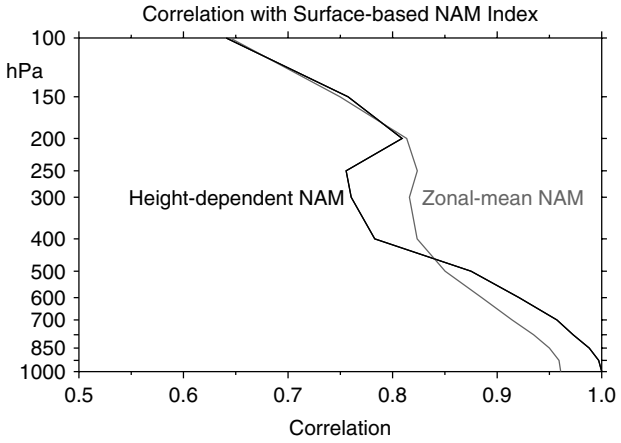

Figure 5. Correlation between the monthly surface-based NAM index and the height-dependent NAM index (black curve). Correlation between the monthly surface-based NAM index and the zonal-mean NAM index (grey curve).

the height-dependent EOF at 300 hPa from Figure 2 (repeated in the bottom left panel of Figure 3) with a linear combination of the patterns in the top panels (shown in the bottom right panel in Figure 3). The linear combination is formed by weighting the top panels by their respective linear regression coefficients with the pattern in the bottom left panel. As evidenced in the bottom panels, the height-dependent NAM at 300 hPa reflects a combination of the first and second EOFs of the 1000 hPa height field (the patterns in the bottom panels are correlated at $r = 0.98$). The contamination of the height-dependent NAM index by the second PC of the 1000 hPa height field peaks at around 300 hPa but is prevalent throughout much of the troposphere and lowermost stratosphere (Figure 4).

In the case of the zonal-mean NAM at 300 hPa (Figure 2, right), the pattern captures the zonally symmetric component of the NAM, but is not contaminated by the PNA pattern (as in the middle panel), and has less distortion over the Atlantic sector due to the effects of surface temperature advection (as in the left panel). The zonal-mean and surface-based patterns bear the strongest resemblance to the 'benchmark' regression and composite maps in Figure 1.

The differences among the three methods are also pronounced in the mid–upper stratosphere (top two rows of Figure 2). The results for the height-dependent and the zonal-mean EOFs are indistinguishable from each other (the pattern correlations exceed 0.99 at 30 and 3 hPa – see Table I). Hence, as is the case at the surface, the leading modes of variability in the zonally varying and zonal-mean stratospheric circulation are largely identical. The results for the surface-based NAM (left) are strikingly different, particularly at 3 hPa. The differences between the left and middle/right panels at 3 hPa are due largely to (1) the lag between variability in the upper stratosphere and the surface (Baldwin and Dunkerton, 1999), and (2) the fact that the structure in the left panel is determined entirely by the covariability with the surface, which is increasingly small with height.

Figure 5 provides additional insight into the differences among the three methodologies. The black line shows the correlations between the height-dependent NAM index at 1000 hPa and the height-dependent NAM index at all levels. The grey line shows the correlations between the height-dependent NAM index at 1000 hPa and the zonal-mean NAM index at all levels. In the case of the height-dependent NAM, the correlations exhibit a pronounced minimum in the upper troposphere. The minimum is also evident in the composites of stratosphere–troposphere coupling presented in Baldwin and Dunkerton (2001). As noted above, the minimum is not physical but rather is an artefact of the mixing of the PNA and NAM in the height-dependent EOFs at those levels.

To gauge which of the three indices provides the best measure of coupling to stratospheric wind anomalies, Figure 6 shows correlations (daily, November–March) between all three indices and the time series of

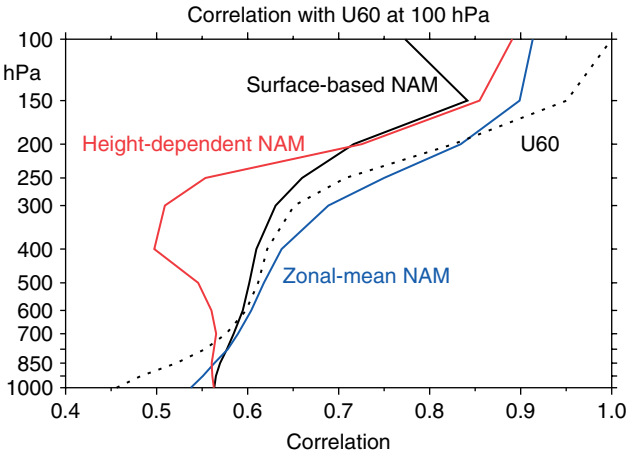

Figure 6. Correlation during November to March between the daily zonal wind anomaly at 60°N, 100 hPa and the surface-based NAM index (black), the height-dependent NAM index (red), and the zonal-mean NAM index (blue). The dotted line shows the correlation between the daily zonal wind at 60°N, 100 hPa with the same quantity at other levels.

DOI: 10.1002/qj

zonal-mean zonal wind anomalies at 60°N and 100 hPa. Consistent with the previous figures, the height-dependent NAM index shows greatly reduced correlations in the upper troposphere. The surface-based NAM indices exhibit higher correlations in the middle troposphere, but the highest correlations are found in association with the zonal-mean NAM index. The only exception is near the surface, where the correlations for the surface and multi-level methods slightly exceed those for the zonal-mean method (0.54 vs. 0.56).

The top two panels in Figure 7 show composites of weak and strong stratospheric events based on the zonal-mean NAM indices; the bottom two panels show analogous results based on the height-dependent NAM

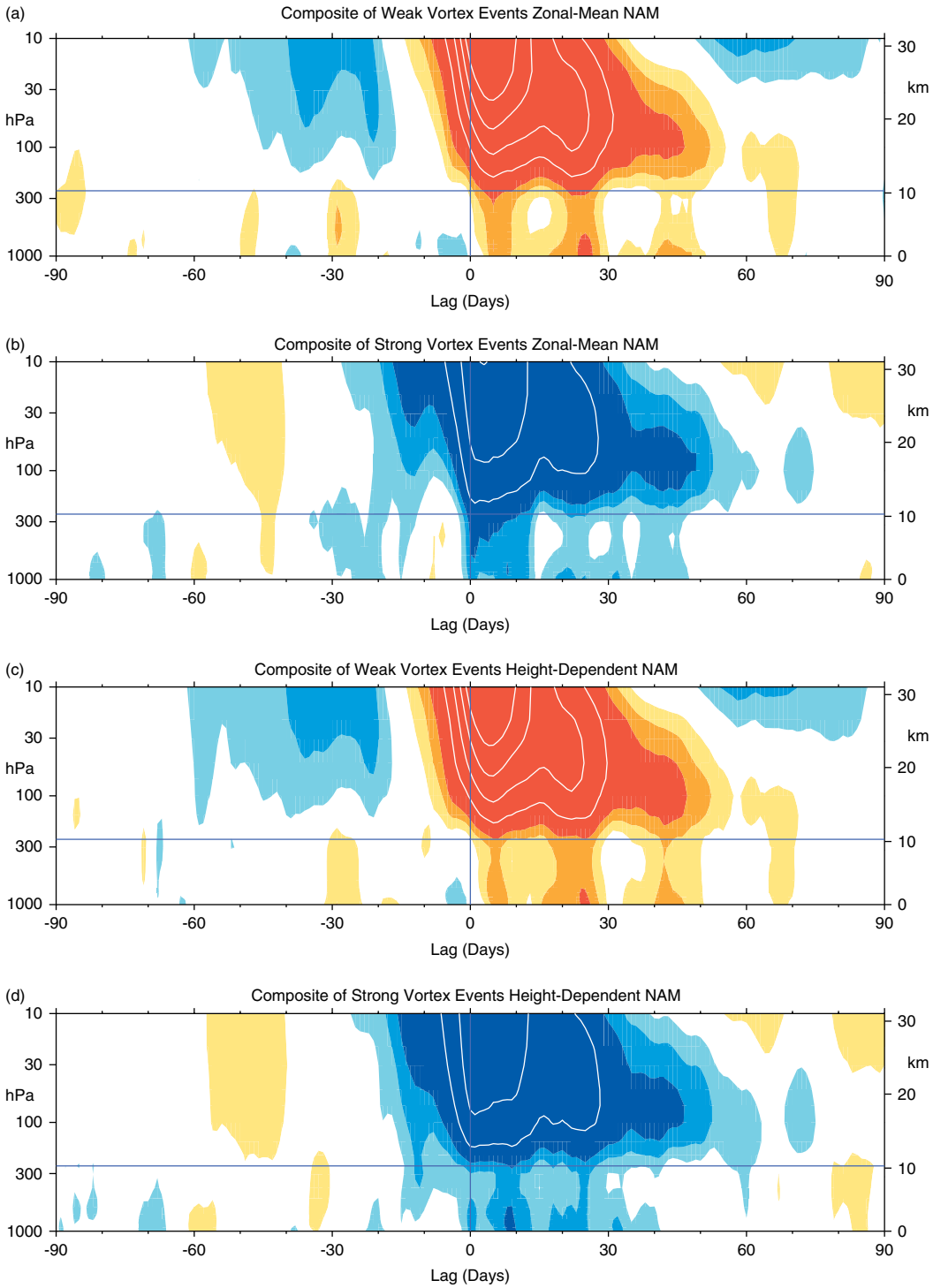

Figure 7. (a) Composites of time–height development of the zonal-mean NAM index for 29 weak vortex events. The events are determined by the dates on which the 10 hPa NAM index exceeded −3.0. The indices are non-dimensional; the contour interval for the colour shading is 0.25, and 0.5 for the white contours. Values between −0.25 and 0.25 are unshaded. The thin horizontal lines indicate the approximate tropopause. The methodology is described in Baldwin and Dunkerton (2001). (b) As in the top panel, but 29 strong vortex events in which the NAM index exceeded 2.0 at 10 hPa. (c) and (d) use the same dates as (a) and (b), but contour the height-dependent NAM index.

DOI: 10.1002/qj

indices (the bottom panels are similar to those shown in Baldwin and Dunkerton (2001)). For the most part, the time/height evolution of the results based on both methods is indistinguishable. However, recall that as noted in Figures 1 and 2, the zonal-mean NAM indices provide tropospheric patterns that are closest to the patterns associated with stratospheric variability.

Figure 8 is analogous to Figure 2, but shows results for the Southern Hemisphere. The results in the left column are based on the leading PC of 1000 hPa geopotential height for all months (1979–2007), but virtually identical results are derived for analyses based on the leading PC time series of the 850 or 500 hPa height field (not shown). In general, the discrepancies among the three methods are much smaller in the Southern Hemisphere than in the Northern Hemisphere, particularly in the upper troposphere. Correlations between pairs of patterns are shown in Table II. As is the case in the Northern Hemisphere, the surface-based method yields degraded structures at stratospheric levels. But unlike the Northern

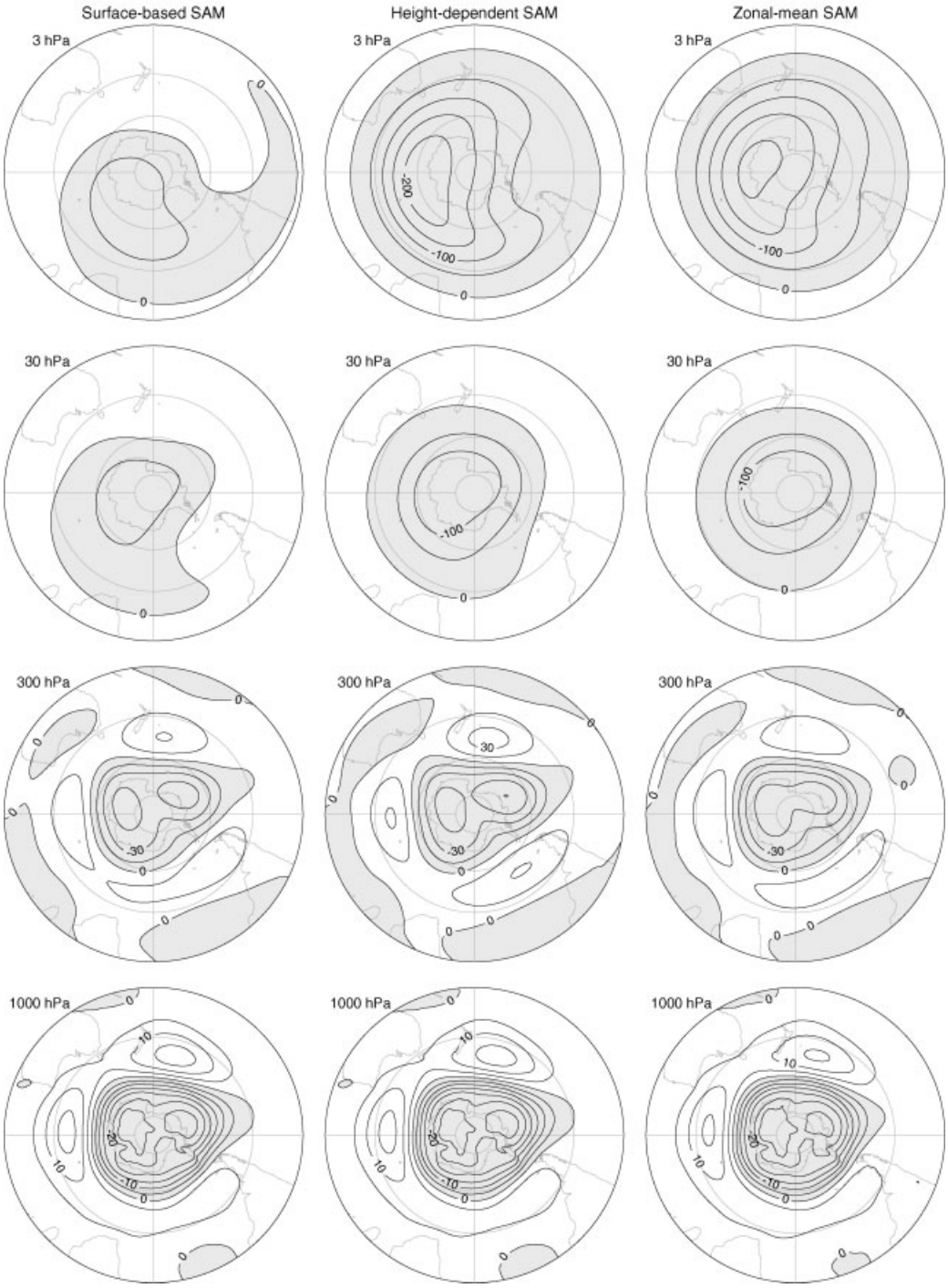

Figure 8. Left column: Spatial patterns of the surface-based SAM, with a base level of 1000 hPa, defined using equation (3) (Thompson and Wallace, 1998, 2000). Centre column: spatial patterns (EOFs) of the height-dependent SAM. Right column: spatial patterns of the zonal-mean SAM, defined using equation (6).

DOI: 10.1002/qj

Table II. Area-weighted spatial correlations between pairs of panels in Figure 8.

	Columns 1–2	Columns 1–3	Columns 2–3
3 hPa	0.581	0.516	0.957
30 hPa	0.906	0.855	0.976
300 hPa	0.990	0.989	0.976
1000 hPa	1.00	0.986	0.986

Hemisphere, both the height-dependent and zonal-mean methods provide consistent representations of annular mode variability throughout the troposphere. Relative to the Northern Hemisphere, the patterns in the Southern Hemisphere are more zonally symmetric, more coherent through the troposphere and stratosphere, and vary less as a function of methodology.

4. Discussion

The results in the previous section reveal three key aspects of the methodologies outlined in section 2:

(1) The *surface-based* definition of the annular modes makes it difficult to generate daily annular mode indices at all levels, but particularly at middle and upper stratospheric levels.
(2) The *height-dependent* methodology is robust at the surface and in the stratosphere, but is not appropriate for generating annular mode indices in the upper troposphere. This is because the height-dependent EOFs in the free troposphere reflect a mix of the two leading EOFs of the near-surface geopotential height field.
(3) The *zonal-mean* methodology minimizes the undesirable aspects of the first two methods for diagnosing stratosphere–troposphere coupling. It is also less dependent on subjective choices, yields higher correlations between variability at stratospheric and tropospheric levels, and requires two orders of magnitude fewer data.

How does the zonal-mean methodology compare to simple indices based on geopotential over the polar cap and zonal wind at a fixed latitude? Cohen *et al.* (2002) approximated the NAM index by averaging geopotential anomalies over the polar cap. As shown in Figure 9, the polar-cap average geopotential anomaly is a good approximation to the zonal-mean NAM index at all levels from the surface to 3 hPa, but is sensitive to the definition of the polar cap. Correlations between daily polar-cap geopotential anomalies and the zonal-mean NAM index are highest when the polar cap boundary is between 60° and 70° in either hemisphere, and peak near 65°. Using 65°N to define the polar cap, the daily correlations between the two indices exceed −0.96 throughout the troposphere and −0.99 in the stratosphere. SAM correlations at 65°S (not shown) are in the −0.91 to −0.99 range. A polar-cap geopotential anomaly (65° to the Pole) is used as a climate diagnostic by the NOAA Climate Prediction Center (www.noaa.cpc.gov).

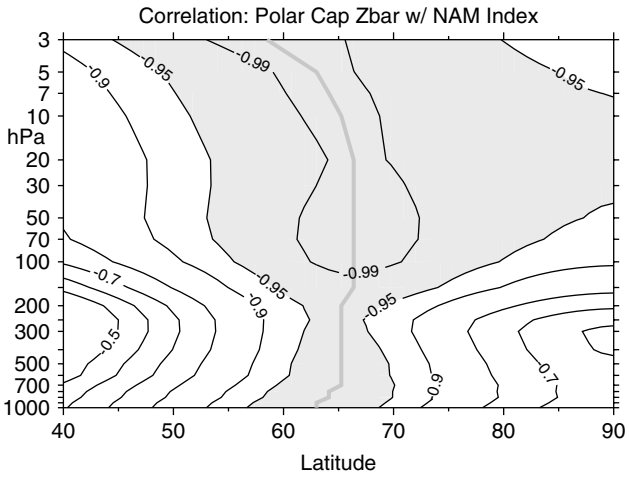

Figure 9. Correlation between the daily zonal-mean NAM index and the area-averaged polar cap geopotential anomaly. The definition of the polar cap ranges from 40°N to 90°N. The grey curve indicates the lower latitude of the polar cap that maximizes the correlation with the NAM index. Values exceeding −0.95 are shaded.

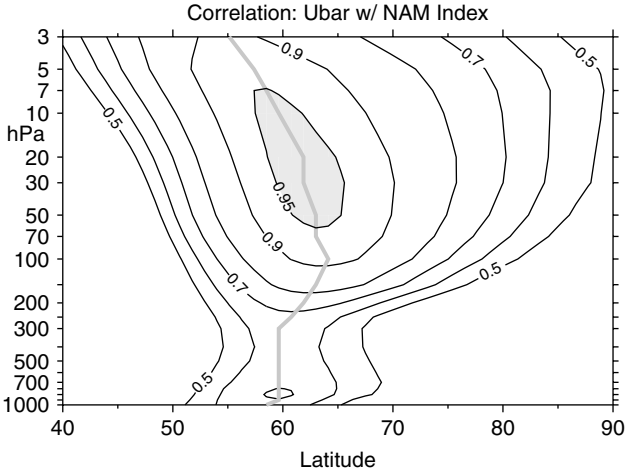

Figure 10. Correlation between the daily zonal-mean NAM index and the corresponding zonal-mean wind anomaly from 40°N to 90°N. The grey curve indicates the latitude of the zonal-mean wind that maximizes the correlation with the NAM index. Values exceeding 0.95 are shaded.

Christiansen (2005, 2009) diagnosed stratosphere–troposphere coupling using the zonal-mean zonal wind at 60°N. As is the case for geopotential height averaged over the polar cap, the zonal-mean zonal wind is a readily observable quantity and is a reasonably good approximation to the zonal-mean NAM index in the stratosphere (Figure 10). But as illustrated in Figure 10, the correlations with the NAM index are less than 0.70 in the troposphere. Furthermore, as indicated by the dotted line in Figure 6, the correlations between the zonal wind at 60°N at 100 hPa and tropospheric levels are lower than those found in association with tropospheric values of the zonal-mean NAM indices. Accordingly, composites of weak and strong stratospheric vortex events based on the zonal wind at 60°N substantially

DOI: 10.1002/qj

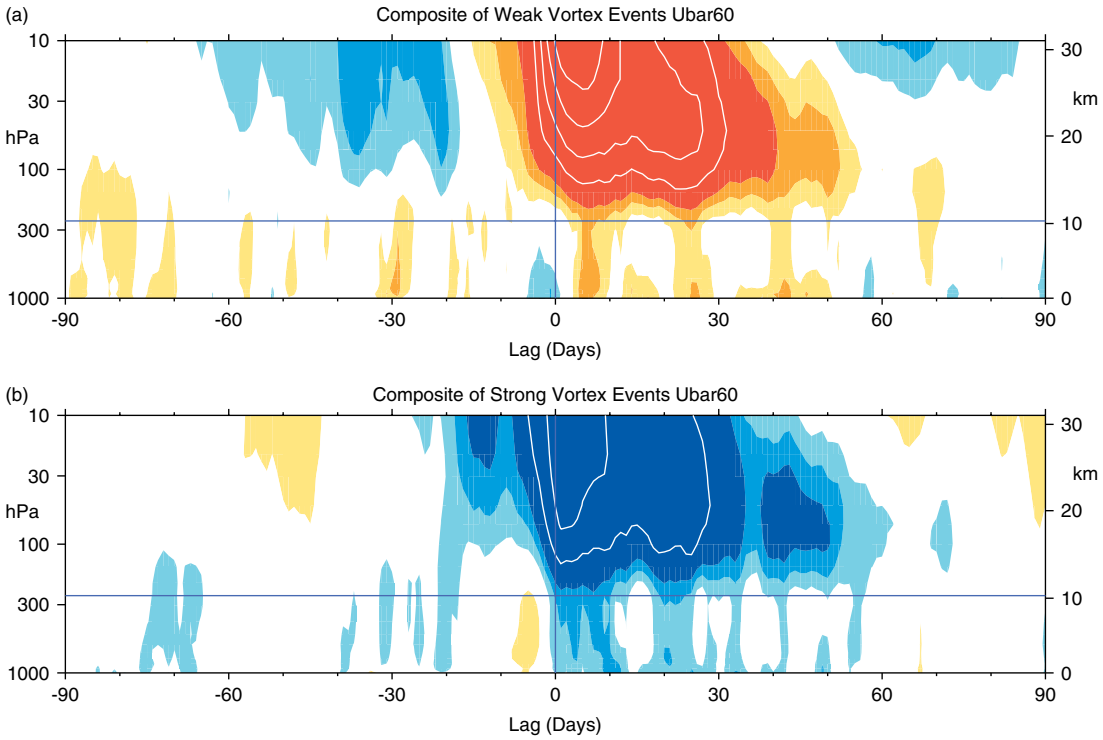

Figure 11. As in Figure 7, except using an index of the zonal-mean wind at 60°N.

underestimate the strength of stratosphere–troposphere coupling as suggested by the NAM indices (compare Figures 11 and 7).

Thus, polar cap-averaged geopotential is an effective substitute for the zonal-mean NAM index. But the optimum latitude of the polar cap boundary is ultimately determined by EOF-based methods, and may vary from climate model to climate model. In this sense, the EOF-based method is more flexible and does not require the justification of an arbitrary choice in defining the polar cap.

A practical argument for the use of the zonal-mean EOF methodology is that model output is seldom available for calculating annular mode indices using the other EOF-based methods. The lack of zonally varying geopotential height output has been an impediment to analysing stratosphere–troposphere coupling in models such as those assessed by the IPCC. We suggest that daily zonal-mean geopotential be standard model output, enabling the calculation of daily annular mode indices and robust model intercomparisons.

The zonal-mean annular mode method can be used to compare observations with models, but attention must be paid to (1) normalizing the indices relative to the observations, and (2) trends in either the observations or model runs. By construction, the zonal-mean method will always yield AM times series with unit variance, regardless of the amplitude of the corresponding spatial patterns. To account for the differences in the modelled and observed amplitudes in the annular modes, the baseline weighted amplitude of the zonal-mean EOF can be defined from observations as $A(z) = RMS(e(z)W)$, where $e(z)$ is the height-dependent latitudinal profile of the EOF, and W is cosine of latitude. The amplitude of the model AM indices can then be scaled by the ratio of $A(z)$ calculated for the model and observed EOFs. Some model runs may have significant annular-mode trends due to prescribed changes in greenhouse gases or other factors. In order that the trends not contaminate the definitions of the annular model patterns and indices, the data may be detrended before calculating the EOF patterns. In this case, the model AM indices are found by projecting the original data onto the EOF patterns using Equation (2).

Acknowledgements

We thank J.M. Wallace and an anonymous referee for insightful reviews. We thank P. Braesicke, P. Canziani, B. Christiansen, J. Cohen, J. Li and I. Watterson for comments on the manuscript. MPB was funded by the National Science Foundation under the US CLIVAR program and the Office of Polar Programs. DWJT was funded by the National Science Foundation Climate Dynamics Program under budget number ATM-0613082.

References

Baldwin MP. 2001. Annular modes in global daily surface pressure. *Geophys. Res. Lett.* **28**: 4115–4118.

Baldwin MP, Dunkerton TJ. 1999. Propagation of the Arctic Oscillation from the stratosphere to the troposphere. *J. Geophys. Res.* **104**: 30937–30946.

Baldwin MP, Dunkerton TJ. 2001. Stratospheric harbingers of anomalous weather regimes. *Science* **294**: 581–584.

Baldwin MP, Stephenson DB, Jolliffe IT. 2009. Spatial weighting and iterative projection methods for EOFs. *J. Climate* **22**: 234–243.

Braesicke P, Pyle JA. 2004. Sensitivity of dynamics and ozone to different representations of SSTs in the Unified Model. *Q. J. R. Meteorol. Soc.* **130**: 2033–2045.
Christiansen B. 2005. Downward propagation and statistical forecast of the near-surface weather. *J. Geophys. Res.* **110**: D14104, DOI:10.1029/2004JD005431.
Christiansen B. 2009. Is the atmosphere interesting? A projection pursuit study of the circulation in the Northern Hemisphere winter. *J. Climate* **22**: 1239–1254.
Cohen J, Salstein D, Saito K. 2002. A dynamical framework to understand and predict the major Northern Hemisphere mode. *Geophys. Res. Lett.* **29**: 1412, DOI:10.1029/2001GL014117.
Gerber EP, Voronin S, Polvani LM. 2008a. Testing the annular mode autocorrelation time scale in simple atmospheric general circulation models. *Mon. Weather Rev.* **136**: 1523–1536.
Gerber EP, Polvani LM, Ancukiewicz D. 2008b. Annular mode time scales in the Intergovernmental Panel on Climate Change Fourth Assessment Report models. *Geophys. Res. Lett.* **35**: L22707, DOI:10.1029/2008GL035712.
Gong D, Wang S. 1999. Definition of Antarctic Oscillation index. *Geophys. Res. Lett.* **26**: 459–462.
Hartmann DL, Lo F. 1998. Wave-driven zonal flow vacillation in the Southern Hemisphere. *J. Atmos. Sci.* **55**: 1303–1315.
Hurrell JW, Kushnir Y, Ottersen G, Visbeck M. 2003. An overview of the North Atlantic Oscillation. Pp 1–35 in *The North Atlantic Oscillation: Climate significance and environmental impact*, Hurrell JW, Kushnir Y, Ottersen G, Visbeck M (eds). *Geophysical Monograph Series*, 134. American Geophysical Union.
Karoly DJ. 1990. The role of transient eddies in low-frequency zonal variations of the Southern Hemisphere circulation. *Tellus* **42A**: 41–50.
Kidson JW. 1988. Indices of the Southern Hemisphere zonal wind. *J. Climate* **1**: 183–194.
Limpasuvan V, Hartmann DL. 2000. Wave-maintained annular modes of climate variability. *J. Climate* **13**: 4414–4429.
Lorenz DJ, Hartmann DL. 2001. Eddy–zonal flow feedback in the Southern Hemisphere. *J. Atmos. Sci.* **58**: 3312–3327.
Lorenz DJ, Hartmann DL. 2003. Eddy–zonal flow feedback in the Northern Hemisphere winter. *J. Climate* **16**: 1212–1227.
Li J, Wang JXL. 2003. A modified zonal index and its physical sense. *Geophys. Res. Lett.* **30**: 1632, DOI:10.1029/2003GL017441.
Marshall GJ. 2003. Trends in the Southern Annular Mode from observations and reanalyses. *J. Climate* **16**: 4134–4143.
Miller RL, Schmidt GA, Shindell DT. 2006. Forced annular variations in the 20th century Intergovernmental Panel on Climate Change Fourth Assessment Report models. *J. Geophys. Res.* **111**: D18101, DOI:10.1029/2005JD006323.
North GR, Bell TL, Cahalan RF, Moeng FJ. 1982. Sampling errors in the estimation of empirical orthogonal functions. *Mon. Weather Rev.* **110**: 699–706.
Norton WA. 2003. Sensitivity of Northern Hemisphere surface climate to simulation of the stratospheric polar vortex. *Geophys. Res. Lett.* **30**: 1627, DOI:10.1029/2003GL016958.
Quadrelli R, Wallace JM. 2004. A simplified linear framework for interpreting patterns of Northern Hemisphere wintertime climate variability. *J. Climate* **17**: 3728–3744.
Thompson DWJ, Solomon S. 2002. Interpretation of recent Southern Hemisphere climate change. *Science* **296**: 895–899.
Thompson DWJ, Wallace JM. 1998. The Arctic Oscillation signature in the wintertime geopotential height and temperature fields. *Geophys. Res. Lett.* **25**: 1297–1300.
Thompson DWJ, Wallace JM. 2000. Annular modes in the extratropical circulation. Part I: Month-to-month variability. *J. Climate* **13**: 1000–1016.
Uppala SM, Kållberg PW, Simmons, AJ, Andrae U, da Costa Bechtold V, Fiorino M, Gibson JK, Haseler J, Hernandez A, Kelly GA, Li X, Onogi K, Saarinen S, Sokka N, Allan RP, Andersson E, Arpe K, Balmaseda MA, Beljaars ACM, van de Berg L, Bidlot J, Bormann N, Caires S, Chevallier F, Dethof A, Dragosavac M, Fisher M, Fuentes M, Hagemann S, Hólm E, Hoskins BJ, Isaksen L, Janssen PAEM, Jenne R, McNally AP, Mahfouf J-F, Morcrette J-J, Rayner NA, Saunders RW, Simon P, Sterl A, Trenberth KE, Untch A, Vasiljevic D, Viterbo P, Woollen J. 2005. The ERA-40 re-analysis. *Q. J. R. Meteorol. Soc.* **131**: 2961–3012.